JOURNAL OF CHEMICAL & ENGINEERING DATA

ARTICLE

pubs.acs.org/jced

Accurate $P-\rho-T$ Data and Phase Boundary Determination for a Synthetic Residual Natural Gas Mixture

Diego E. Cristancho, Ivan D. Mantilla, L. Alejandro Coy, Andrea Tibaduiza, Diego O. Ortiz-Vega, and Kenneth R. Hall*

Artie McFerrin Department of Chemical Engineering, Texas A&M University, College Station, Texas 77843-3122, United States

Gustavo A. Iglesias-Silva

Departamento de Ingeniería Química, Instituto Tecnológico de Celaya, Celaya, México

ABSTRACT: This paper reports $P-\rho-T$ data (P is pressure, ρ is mass density, T is temperature) for a ternary mixture that resembles a residual natural gas. The measurements utilized a high-pressure, single-sinker magnetic-suspension densimeter (MSD) from (200 to 450) K up to 170 MPa and an automated isochoric apparatus to determine densities and phase boundary data up to 20 MPa. The MSD technique yielded accurate data, with better than a 0.05 % estimated error at two standard deviations up to 200 MPa. The relative uncertainties for phase-boundary temperatures and pressures were 0.45 % and 0.04 %, respectively. The isochoric densities had essentially the same estimated error as the MSD data. The GERG-2004 and AGA8-DC92 equations of state compared well to the density data. A new method provided saturation densities from isochoric data with a relative uncertainty of 0.12 %, compensating the isochoric densities for cell and transfer-line volume changes and for mass interchange between the cell and the combination of the transfer line and pressure transducer.

INTRODUCTION

Residual (or pipeline) natural gas is a principal product of a natural gas processing plant. Its importance as an energy source for industrial process, residential and commercial uses, transportation, and generation of electric power is unquestionable.[1] Although its composition is variable, a ternary mixture of methane, ethane, and propane is a suitable surrogate for densities. Accurate characterization of the densities of such mixtures has been a fundamental research problem for many years.[2,3] Accurate $P-\rho-T$ data combined with experimental phase boundaries are necessary for the development and validatation of reference equations of state (EOS).[4]

Over the past 20 years, new reference EOS for the main components of natural gas have appeared.[5−9] The Thermodynamics Laboratory at Texas A&M University has recently produced new, highly accurate data at high pressure for methane,[5] ethane,[6] nitrogen,[7] and carbon dioxide[8] using a single-sinker magnetic-suspension densimeter (MSD). These data have demonstrated that the fundamental EOS used as reference standards for these compounds[9] behave well at high pressures. This paper presents new $P-\rho-T$ data for a ternary mixture that resembles a residual natural gas as part of a systematic study to validate and support natural gas standard EOS such as AGA8-DC92[10] and GERG-2004[2] at high pressure.

In addition, this paper provides equilibrium data and densities measured with a low-pressure isochoric apparatus. The Peng−Robinson[11] EOS results are compared with the phase-boundary data because the industry commonly uses this EOS for phase equilibrium calculations. This work employed a phase-behavior simulator developed in the Thermodynamics Laboratory. Finally, the paper proposes and applies a new methodology for predicting saturation densities using isochoric data.

EXPERIMENTAL SECTION

This paper presents isothermal density data for a ternary mixture at (300, 350, and 400) K up to 170 MPa as well as equilibrium data. DCG PARTNERSHIP Inc. prepared the ternary mixture gravimetrically with mole fractions of 0.95039, 0.03961, and 0.01000 for methane, ethane, and propane, respectively, with an estimated gravimetric uncertainty of ± 0.04 % (NIST-traceable by weight). The MSD uses Archimedes' principle to determine densities by weighing a sinker in vacuum and the again in a sample fluid. The significant feature of the apparatus is that the balance and the sinker are coupled magnetically rather than physically, thus allowing wider ranges of temperature and pressure measurements with less regard for the chemical characteristics of the sample fluid. The titanium sinker mass and volume were 30.39159 g and 6.741043 cm^3, respectively, as determined using the apparatus and procedure described by McLinden and Splett.[12] Patil and co-workers[13,14] have described the single-sinker MSD used in this work. Modifications to expand the range of measured temperature have appeared in the

Special Issue: John M. Prausnitz Festschrift

Received: May 11, 2010
Accepted: July 4, 2010
Published: July 27, 2010

ACS Publications © 2010 American Chemical Society

Table 1. MSD Densities

	ρ/kg·m^{-3}				
P/MPa	exptl	GERG-2004	AGA8-DC92	$100\cdot(\rho - \rho_{GERG})/\rho$	$100\cdot(\rho - \rho_{AGA8})/\rho$
			T = 300.000 K		
4.965	36.976	36.988	36.991	−0.032	−0.040
5.998	45.559	45.570	45.574	−0.023	−0.032
6.994	54.107	54.122	54.125	−0.027	−0.032
8.002	63.008	63.024	63.028	−0.025	−0.032
9.998	81.252	81.275	81.278	−0.028	−0.032
12.427	103.999	104.020	104.030	−0.020	−0.029
14.992	127.615	127.640	127.640	−0.019	−0.019
20.017	168.796	168.810	168.780	−0.008	0.009
25.012	200.944	200.940	200.910	0.002	0.017
30.021	225.761	225.740	225.710	0.009	0.023
44.944	274.513	274.470	274.350	0.016	0.059
49.920	285.997	285.970	285.820	0.010	0.062
50.254	286.701	286.680	286.540	0.007	0.056
			T = 350.000 K		
2.002	11.854	11.857	11.857	−0.024	−0.024
4.998	30.447	30.452	30.455	−0.017	−0.027
10.001	63.246	63.251	63.263	−0.007	−0.026
19.987	128.080	128.070	128.090	0.008	−0.008
30.019	180.470	180.460	180.410	0.006	0.033
39.996	218.303	218.300	218.280	0.001	0.011
49.953	246.399	246.350	246.320	0.020	0.032
69.915	286.052	286.050	285.960	0.001	0.032
79.946	301.044	301.060	300.940	−0.005	0.035
99.921	325.172	325.190	325.060	−0.006	0.034
119.976	344.390	344.400	344.270	−0.003	0.035
139.909	360.259	360.240	360.150	0.005	0.030
149.927	367.348	367.310	367.240	0.010	0.030
169.848	380.063	379.990	379.970	0.019	0.025
			T = 400.000 K		
4.999	25.994	25.993	25.996	0.003	−0.008
10.004	52.804	52.802	52.814	0.003	−0.019
19.992	104.944	104.920	104.960	0.023	−0.015
30.035	150.199	150.170	150.170	0.019	0.019
40.009	186.143	186.130	186.090	0.007	0.028
49.929	214.526	214.470	214.450	0.026	0.035
59.959	237.631	237.590	237.600	0.017	0.013
69.948	256.657	256.640	256.640	0.006	0.006
79.919	272.755	272.750	272.740	0.002	0.005
89.963	286.787	286.790	286.760	−0.001	0.009
99.971	299.071	299.080	299.030	−0.003	0.014
119.622	319.587	319.580	319.510	0.002	0.024
139.783	337.056	337.020	336.940	0.011	0.035

literature.[15,16] A Minco Products model S1059PA5X6 platinum resistance thermometer (PRT) with calibration at fixed temperature points defined by ITS-90 and by a calibrated PRT traceable to NIST was used. The temperature stability was ± 5 mK, and the uncertainty of the PRT was 2 mK with respect to the triple point of water.[15,16] Two Digiquartz transducers (40 and 200 MPa, Paroscientific Inc.) were used to measure pressure. The uncertainty for these transducers was 0.01 % of full scale.

The characteristics of the low-pressure isochoric apparatus appear in previous reports by Zhou and co-workers.[17,18] The pressure and temperature transducers in this apparatus have the same uncertainties as those for the MSD, but this apparatus can operates up to only 21 MPa. Acosta-Perez et al.[19] have described the methodology for determining the phase boundaries using isochoric data, which involves determining the change in slope of the isochore as it crosses the phase boundary. The estimated

dx.doi.org/10.1021/je100500t |J. Chem. Eng. Data 2011, 56, 826–832

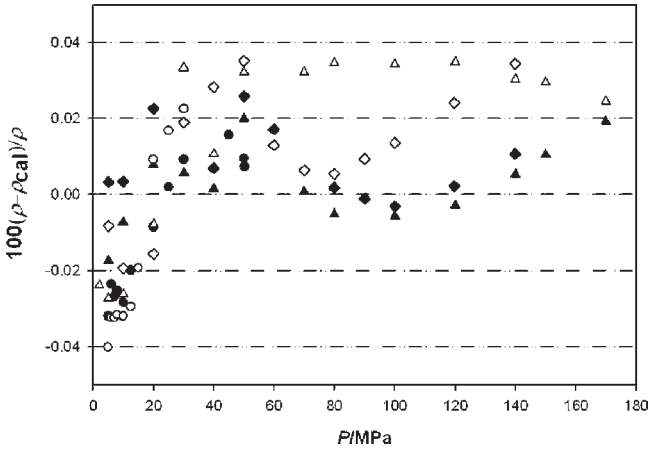

Figure 1. Percentage deviations of the experimental $P-\rho-T$ data from values calculated using the GERG-2004 and AGA8-DC92[10] equations of state. GERG-2004: ●, 300.000 K; ▲, 350.000 K; ◆, 400.000 K. AGA8-DC92: ○, 300.000 K; △, 350.000 K; ◇ 400.000 K.

Table 2. Second and Third Virial Coefficients

T/K	B/cm^3·mol^{-1}	C/cm^6·mol^{-2}
300.000	−47.5407	2638.812
350.000	−31.0707	2539.004
400.000	−19.437	2338.606

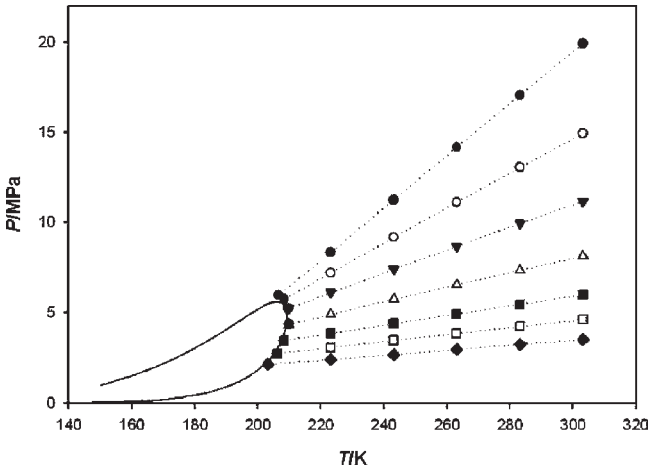

Figure 2. Isochoric experimental design: ●, isochore 1; ○, isochore 2; ▼, isochore 3; △, isochore 4; ■, isochore 5; □, isochore 6; ◆, isochore 7; —, Peng−Robinson EOS.

uncertainties for a temperature and pressure phase-boundary point were 0.45 % and 0.04 %, respectively.

■ RESULTS AND ANALYSIS

The density data for the sample and their comparisons to GERG-2004 and AGA8-DC92 predictions (implemented in REFPROP 8.0[9]) appear in Table 1, and Figure 1 illustrates the deviations. This figure indicates that GERG-2004 has better predictive capability across the range of pressure than AGA8-DC92. GERG-2004 predicted the density data with an uncertainty of approximately 0.02 % up to 170 MPa. This result is consistent with those found previously for pure-component

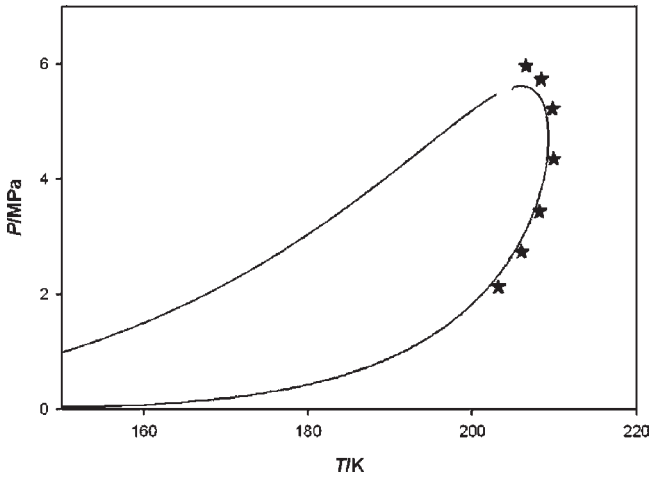

Figure 3. Experimental phase boundary: ★, experimental data; —, Peng−Robinson EOS.

Table 3. Binary Interaction Parameters for the Peng−Robinson EOS Determined in This Laboratory[a]

methane−ethane	−0.0021
methane−propane	−0.0029
ethane−propane	0.008

[a] Unpublished data.

density data at high pressure.[5,6] Therefore, it appears that the approach recently developed by different authors[2,4−8] to construct multiparameter EOS can predict high-pressure density data with excellent accuracy, at least up to ∼200 MPa. AGA8-DC92 exhibited an uncertainty of 0.04 % across the pressure range. The procedure described by Cristancho et al[5] [i.e., fitting $(Z-1)/\rho$ in the linear region to determine the intercept and slope] was used to obtain the second and third virial coefficients, which appear in Table 2. The estimated absolute uncertainties for the second and third virial coefficients are 0.57 cm^3·mol^{-1} and 125 cm^6·mol^{-2}, respectively.

The procedure of using the change in slope of isochores to determine phase boundaries has appeared previously.[17−19] Figure 2 represents the experimental procedure, and Figure 3 presents the phase boundary data. The predicted phase envelope that appears in Figure 2 was calculated using the Peng−Robinson EOS with binary interaction parameters determined from the equilibrium data for natural gas mixtures presented in Table 3. The equation predictions followed the trend of the experimental data, but the deviations increase when approaching the cricondenbar. Because the experiment was neither exactly isochoric nor isomolar, this paper presents a new methodology to compensate for these effects and determine the saturation density.

Isochoric and Saturated Density Determination. These two effects require compensation to determine density using isochoric data and phase boundaries. First, a volume change with temperature and pressure exists in the sample cell, in the transmission line between the isochoric cell and the pressure transducer, and in the transducer. This effect is related to the thermomechanical properties of the materials used for the cell (c), transmission line (l), and transducer (t):

$$\frac{V(T,P)}{V_{\mathrm{ref}}(T_{\mathrm{ref}},P_{\mathrm{ref}})} = 1+\beta(T-T_{\mathrm{ref}})+\kappa(P-P_{\mathrm{ref}}) \qquad (1)$$

dx.doi.org/10.1021/je100500t |J. Chem. Eng. Data 2011, 56, 826–832

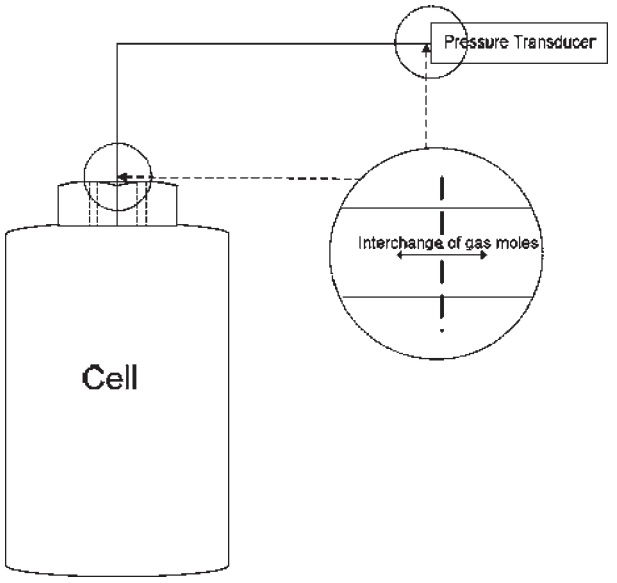

Figure 4. Schematic diagram showing the mass interchange in the low-pressure isochoric apparatus.

Table 4. Low-Pressure Isochoric Apparatus Parameters[a]

V^{c}_{ref}/m^3	$6.01 \cdot 10^{-5}$
V^{l}_{ref}/m^3	$7.32 \cdot 10^{-9}$
V^{t}_{ref}/m^3	$2.05 \cdot 10^{-7}$
$\kappa_c, \kappa_l, \kappa_t/MPa^{-1}$	$4.86 \cdot 10^{-5}$
$\beta_c, \beta_l, \beta_t/K^{-1}$	$2.53 \cdot 10^{-5}$
T_{ref}/K	298.15
P_{ref}/MPa	0.101325
T_l/K	333.15
T_t/K	343.15

[a] The material of the isochoric cell, transmission line, and pressure transducer is stainless steel.

where V is the total volume, β is the thermal expansion coefficient, κ is the pressure distortion parameter, and "ref" subscripts refer to the reference conditions.

In addition, amounts of material move between the sample cell, the transmission line, and the transducer during the experiment, and the phenomenon is a function of the various pressures and temperatures. Figure 4 illustrates the apparatus. Compensation for this effect requires a model. The amount balance is

$$n_T = n_c + n_l + n_t \quad (2)$$

where n_T is the total number of moles, n_c is the number of moles in the cell, n_l is the number of moles in the transmission line, and n_t is the number of moles in the transducer. Substituting the real-gas equation $n = PV/RTZ$, where R is the gas constant and Z is the real-gas factor, into eq 2 gives

$$n_T = \frac{PV_c}{RT_cZ_c} + \frac{PV_l}{RT_lZ_l} + \frac{PV_t}{RT_tZ_t} \quad (3)$$

When eq 1 for the volumes is used along with the fact that the temperatures of the transmission line and transducer are constant during the experiment, eq 3 becomes:

$$n_T = \frac{P}{T}\left\{\frac{V^{c}_{ref}[1+\beta_c(T_c - T_{ref}) + \kappa_c(P_c - P_{ref})]}{T_cZ_c} + \frac{V^{l}_{ref}[1+\beta_l(T_l - T_{ref}) + \kappa_l(P_l - P_{ref})]}{T_lZ_l} + \frac{V^{t}_{ref}[1+\beta_t(T_t - T_{ref}) + \kappa_t(P_t - P_{ref})]}{T_tZ_t}\right\} \quad (4)$$

The unknown parameters in eq 4 are V^{c}_{ref}, V^{l}_{ref}, V^{t}_{ref}, and n_T. The value of n_T is different for each set of isochoric data. The Z factor is available from the MSD $P-\rho-T$ data or a reliable EOS such as GERG-2004[2] (the data would take precedence). The unknown

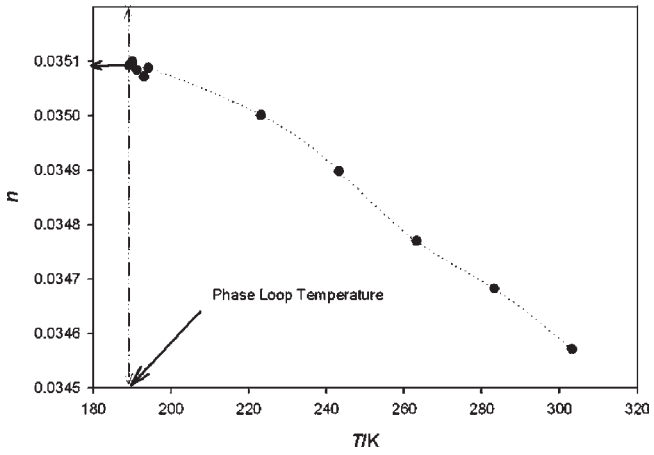

Figure 5. Methodology for determining the number of moles in the calculation of saturation density.

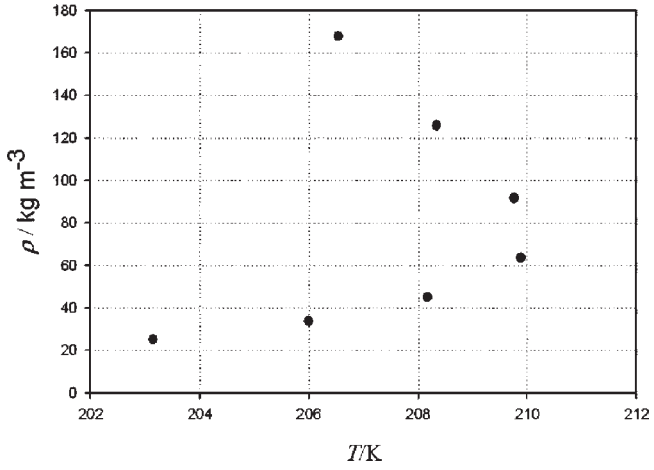

Figure 6. Saturation density−temperature diagram.

Table 5. Phase Boundary Data

T/K	P/MPa	$\rho^{sat}/kg \cdot m^{-3}$
206.540	5.972	165.779
208.340	5.734	125.294
209.756	5.224	90.963
209.879	4.350	63.619
208.174	3.436	45.158
205.999	2.735	33.847
203.150	2.127	25.282

dx.doi.org/10.1021/je100500t |J. Chem. Eng. Data 2011, 56, 826–832

Table 6. $P-\rho-T$ Isochoric Data

T/K	P/MPa	V_c/cm^3	n_c/mol	ρ_{iso}/kg·m^{-3}	ρ_{ref}[a]/kg·m^{-3}	$100\cdot(\rho_{iso}-\rho_{ref})/\rho_{iso}$
			Isochore 1 (n_T = 0.5883 mol)			
303.150	19.908	60.2	0.5866	164.601	164.626	−0.02
283.150	17.046	60.1	0.5869	164.838	164.917	−0.05
263.150	14.157	60.0	0.5871	165.080	165.158	−0.05
243.150	11.250	60.0	0.5874	165.324	165.342	−0.01
223.150	8.340	59.9	0.5876	165.569	165.469	0.06
209.150	6.342	59.9	0.5878	165.739	167.575	−1.11
208.650	6.278	59.9	0.5878	165.745	168.314	−1.55
208.150	6.203	59.9	0.5878	165.751	168.175	−1.46
207.150	6.063	59.9	0.5878	165.763	168.784	−1.82
			Isochore 2 (n_T = 0.4448 mol)			
303.150	14.927	60.1	0.4435	124.459	124.339	0.096
283.150	13.034	60.1	0.4437	124.632	124.565	0.054
263.150	11.115	60.0	0.4438	124.807	124.729	0.062
243.151	9.167	60.0	0.4440	124.982	124.743	0.192
223.150	7.224	59.9	0.4442	125.158	125.686	−0.422
213.150	6.219	59.9	0.4443	125.246	125.808	−0.449
212.150	6.114	59.9	0.4443	125.255	125.609	−0.283
211.150	6.013	59.9	0.4443	125.264	125.642	−0.302
210.150	5.916	59.9	0.4443	125.273	125.952	−0.542
209.150	5.821	59.9	0.4443	125.281	126.462	−0.943
			Isochore 3 (n_T = 0.3230 mol)			
303.150	11.166	60.1	0.3221	90.390	90.351	0.044
283.150	9.933	60.1	0.3222	90.511	90.513	−0.002
263.150	8.678	60.0	0.3223	90.633	90.610	0.025
243.150	7.406	60.0	0.3224	90.755	90.746	0.010
223.150	6.112	59.9	0.3225	90.877	91.055	−0.196
213.150	5.452	59.9	0.3226	90.938	91.403	−0.511
211.650	5.350	59.9	0.3226	90.947	91.409	−0.508
211.150	5.317	59.9	0.3226	90.950	91.453	−0.553
210.650	5.284	59.9	0.3226	90.954	91.5	−0.601
210.150	5.249	59.9	0.3226	90.957	91.470	−0.564
			Isochore 4 (n_T = 0.2260 mol)			
303.150	8.147	60.1	0.225	63.234	63.206	0.044
283.150	7.357	60.1	0.225	63.315	63.284	0.050
263.150	6.557	60.0	0.225	63.397	63.364	0.053
243.150	5.746	60.0	0.226	63.480	63.474	0.009
223.150	4.915	59.9	0.226	63.562	63.563	−0.002
214.150	4.534	59.9	0.226	63.599	63.633	−0.053
213.650	4.512	59.9	0.226	63.601	63.623	−0.034
213.150	4.491	59.9	0.226	63.603	63.636	−0.051
212.650	4.470	59.9	0.226	63.606	63.650	−0.070
212.150	4.448	59.9	0.226	63.608	63.641	−0.052
211.650	4.427	59.9	0.226	63.610	63.656	−0.073
211.150	4.405	59.9	0.226	63.612	63.648	−0.057
210.650	4.384	59.9	0.226	63.614	63.664	−0.079
210.150	4.363	59.9	0.226	63.616	63.682	−0.104
			Isochore 5 (n_T = 0.1604 mol)			
303.150	5.999	60.1	0.1599	44.886	44.877	0.020
283.150	5.473	60.1	0.1600	44.943	44.921	0.048
263.151	4.944	60.0	0.1600	44.999	44.995	0.010
243.150	4.405	60.0	0.1600	45.056	45.045	0.025

dx.doi.org/10.1021/je100500t |J. Chem. Eng. Data 2011, 56, 826–832

Table 6. Continued

T/K	P/MPa	V_c/cm^3	n_c/mol	ρ_{iso}/kg·m^{-3}	ρ_{ref}[a]/kg·m^{-3}	$100\cdot(\rho_{iso}-\rho_{ref})/\rho_{iso}$
223.150	3.859	59.9	0.1601	45.113	45.143	−0.066
212.150	3.550	59.9	0.1601	45.145	45.159	−0.031
211.650	3.535	59.9	0.1601	45.147	45.145	0.003
211.150	3.521	59.9	0.1601	45.148	45.148	0.000
210.650	3.506	59.9	0.1601	45.149	45.134	0.034
210.150	3.492	59.9	0.1601	45.151	45.138	0.028
209.150	3.464	59.9	0.1601	45.154	45.148	0.013
			Isochore 6 (n_T = 0.1202 mol)			
303.150	4.613	60.1	0.1199	33.642	33.655	−0.040
283.150	4.236	60.1	0.1199	33.683	33.695	−0.034
263.150	3.856	60.0	0.1199	33.725	33.743	−0.053
243.150	3.468	60.0	0.1199	33.767	33.755	0.036
223.150	3.075	59.9	0.1200	33.809	33.772	0.110
211.650	2.847	59.9	0.1200	33.834	33.803	0.091
211.150	2.838	59.9	0.1200	33.835	33.819	0.046
210.650	2.828	59.9	0.1200	33.836	33.820	0.047
210.150	2.817	59.9	0.1200	33.837	33.806	0.091
209.150	2.798	59.9	0.1200	33.839	33.825	0.041
208.650	2.788	59.9	0.1200	33.840	33.827	0.038
208.151	2.779	59.9	0.1200	33.841	33.844	−0.009
207.150	2.758	59.8	0.1200	33.843	33.833	0.030
206.150	2.738	59.8	0.1200	33.845	33.838	0.021
			Isochore 7 (n_T = 0.0898 mol)			
303.150	3.517	60.1	0.0895	25.127	25.144	−0.067
283.150	3.245	60.1	0.0895	25.158	25.175	−0.068
263.150	2.969	60.0	0.0896	25.189	25.191	−0.008
243.150	2.690	60.0	0.0896	25.220	25.201	0.074
223.151	2.413	59.9	0.0896	25.251	25.273	−0.088
213.150	2.267	59.9	0.0896	25.266	25.239	0.108
211.150	2.240	59.9	0.0896	25.269	25.262	0.030
210.150	2.225	59.9	0.0896	25.271	25.255	0.063
209.650	2.218	59.9	0.0896	25.272	25.258	0.055
209.150	2.211	59.9	0.0896	25.273	25.261	0.046
208.650	2.204	59.9	0.0896	25.273	25.264	0.037
208.154	2.197	59.9	0.0896	25.274	25.266	0.032
207.150	2.183	59.8	0.0896	25.276	25.273	0.011
206.150	2.169	59.8	0.0896	25.277	25.280	−0.011
205.150	2.155	59.8	0.0896	25.279	25.287	−0.032
204.150	2.141	59.8	0.0896	25.280	25.295	−0.058

[a] Calculated using REFPROP 8.0.

parameters in eq 4 are obtained by fitting the isochoric data. Table 4 contains the low-pressure isochoric apparatus parameters. The error introduced during this step corresponds to approximately 30 ppm in density. Determination of saturation densities (ρ^{sat}) requires the number of moles in the cell as a function of temperature; extrapolation to the corresponding isochoric temperature provides the saturation value, as shown in Figure 5. Finally, with the number of moles in the cell corresponding to the phase boundary temperature and the volume of the cell, the saturation density is

$$\rho^{sat} = \frac{n_c^{sat}}{V(T^{sat}, P^{sat})} \quad (5)$$

where T^{sat} and P^{sat} are the phase-boundary temperature and pressure. Figure 6 presents the temperature dependence of the saturation densities. The experimental saturation data appear in Table 5. The estimated uncertainty in the saturation densities is 0.12 %.

The procedure for determining saturation densities also applies to the calculation of isochoric densities. The isochoric $P-\rho-T$ data for seven different isochores and their comparisons to values computed using REFPROP 8.0 appear in Table 6, and the deviations are shown in Figure 7. This figure indicates that the EOS density deviations increase near the cricondenbar of the mixture. The EOS isochoric densities appear to have deviations of 0.1 % for pressures distant from the cricondenbar.

dx.doi.org/10.1021/je100500t |J. Chem. Eng. Data 2011, 56, 826–832

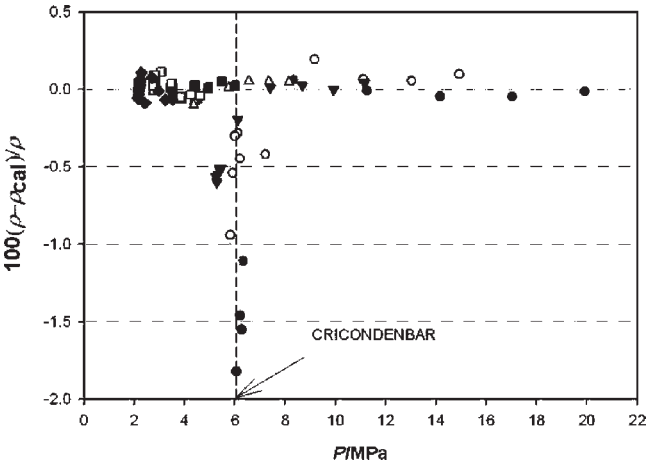

Figure 7. Relative deviations of the experimental isochoric densities and values obtained using the REFPROP 8.0 EOS: ●, isochore 1; ○, isochore 2; ▼, isochore 3; △, isochore 4; ■, isochore 5; □, isochore 6; ◆, isochore 7.

CONCLUSIONS

This paper has reported accurate experimental $P-\rho-T$ data for a residual natural gas mixture using a high-pressure, single-sinker MSD with an experimental uncertainty of less than $5 \cdot 10^{-4}\ \rho$. Virial coefficients have been obtained by extrapolating the $P-\rho-T$ data to zero density. With the isochoric technique including corrections for the volume change and mass interchange, the experimental phase boundary was determined with estimated relative uncertainties of 0.45 %, 0.04 %, and 0.12 % for temperature, pressure, and saturated density data, respectively.

AUTHOR INFORMATION

Corresponding Author

*E-mail: krhall@tamu.edu. Phone: (979) 845 3357. Fax: (979) 845 6446

Funding Sources

The authors gratefully acknowledge support for this work from the Jack E. & Frances Brown Chair Endowment, the Qatar National Research Fund (QNRF) via the National Priorities Research Program (NPRP), and the Texas Engineering Experiment Station.

REFERENCES

(1) *Annual Energy Review 2009*; Energy Information Administration, U.S. Department of Energy: Washington, D.C., 2009.

(2) Kunz, O.; Klimeck, R.; Wagner, W.; Jaeschke, M. The GERG-2004 Wide-Range Equation of State for Natural Gases and Other Mixtures.; *Fortschritt-Berichte VDI, Reihe 6*, No. 557; VDI Verlag GmbH: Düsseldorf, Germany, 2007.

(3) *Orifice Metering of Natural Gas and Other Related Hydrocarbon Fluids*; American Gas Association: Washington, D.C., 2000.

(4) Lemmon, E. W.; Jacobsen, R. T. A Generalized Model for the Thermodynamic Properties of Mixtures. *Int. J. Thermophys.* **1999**, *20*, 825–835.

(5) Cristancho, D. E.; Mantilla, I. D.; Ejaz, S.; Hall, K. R.; Atilhan, M.; Iglesias-Silva, G. A. Accurate $P\rho T$ Data for Methane from (300 to 450) K up to 180 MPa. *J. Chem. Eng. Data* **2010**, *55*, 826–829.

(6) Cristancho, D. E.; Mantilla, I. D.; Ejaz, S.; Hall, K. R.; Atilhan, M.; Iglesias-Silva, G. A., Accurate $P\rho T$ Data for Ethane from (298 to 450) K up to 200 MPa. *J. Chem. Eng. Data* [Online early access]. DOI: 10.1021/je900978x. Published Online: Jan 14, 2010.

(7) Mantilla, I. D.; Cristancho, D. E.; Ejaz, S.; Hall, K. R.; Atilhan, M.; Iglesias-Silva, G. A., Accurate $P-\rho-T$ Data for Nitrogen from (265 to 450) K up to 150 MPa. *J. Chem. Eng. Data* [Online early access]. DOI: 10.1021/je100381g. Published Online: May 19, 2010.

(8) Mantilla, I. D.; Cristancho, D. E.; Ejaz, S.; Hall, K. R.; Atilhan, M.; Iglesias-Silva, G. A., $P-\rho-T$ Data for Carbon Dioxide from (310 to 450) K up to 160 MPa. *J. Chem. Eng. Data* [Online early access]. DOI: 10.1021/je1001158. Published Online: March 31, 2010.

(9) Lemmon, E. W.; Huber, M. L.; McLinden, M. O. *NIST Standard Reference Database 23: Reference Fluid Thermodynamic and Transport Properties—REFPROP*, version 8.0; National Institute of Standards and Technology: Gaithersburg, MD, 2007.

(10) Starling, K. E.; Savidge, J. L. *Compressibility Factors of Natural Gas and Other Related Hydrocarbon Gases*; American Gas Association: Arlington, VA, 1992.

(11) Peng, D.; Robinson, D. B. New Two-Constant Equation of State. *Ind. Eng. Chem. Fundam.* **1976**, *15*, 59–64.

(12) McLinden, M. O.; Splett, J. D. A Liquid Density Standard Over Wide Ranges of Temperature and Pressure Based on Toluene. *J. Res. Natl. Inst. Stand. Technol.* **2008**, *113*, 29–67.

(13) Patil, P.; Ejaz, S.; Atilhan, M.; Cristancho, D.; Holste, J. C.; Hall, K. R. Accurate density measurements for a 91% methane natural gas-like mixture. *J. Chem. Thermodyn.* **2007**, *39*, 1157–1163.

(14) Patil, P. V. Commissioning of a Magnetic Suspension Densitometer for High-Accuracy Density Measurements of Natural Gas Mixtures. Ph.D. Dissertation, Texas A&M University, College Station, TX, 2005.

(15) Ejaz, S. High-Accuracy $P-\rho-T$ Measurements of Pure Gas and Natural Gas Like Mixtures Using a Compact Magnetic Suspension Densimeter. Ph.D. Dissertation, Texas A&M University, College Station, TX, 2007.

(16) Atilhan, M. High-Accuracy $P-\rho-T$ Measurements up to 200 MPa between 200 to 500 K Using a Single Sinker Magnetic Suspension Densitometer for Pure and Natural Gas Like Mixtures. Ph.D. Dissertation, Texas A&M University, College Station, TX, 2005.

(17) Zhou, J.; Patil, P.; Ejaz, S.; Atilhan, M.; Holste, J. C.; Hall, K. R. (p, V_m, T) and Phase Equilibrium Measurements for a Natural Gas-like Mixture Using an Automated Isochoric Apparatus. *J. Chem. Thermodyn.* **2006**, *38*, 1489–1494.

(18) Zhou, J. Automated Isochoric Apparatus for pVT and Phase Equilibrium Measurements on Gas Mixtures. Ph.D. Dissertation, Texas A&M University, College Station, TX, 2005.

(19) Acosta-Perez, P. L.; Cristancho, D. E.; Mantilla, I. D.; Hall, K. R.; Iglesias-Silva, G. A. Method and Uncertainties To Determine Phase Boundaries from Isochoric Data. *Fluid Phase Equilib.* **2009**, *283*, 17–21.